IEEE Access
Multidisciplinary | Rapid Review | Open Access Journal

Received January 25, 2020, accepted February 7, 2020, date of publication February 14, 2020, date of current version February 25, 2020.

Digital Object Identifier 10.1109/ACCESS.2020.2974012

A Diagnosing Method for Phased Antenna Array Element Excitation Amplitude and Phase Failures Using Random Binary Matrices

CAN XIONG, (Student Member, IEEE), AND GAOBIAO XIAO, (Member, IEEE)
Key Laboratory of Ministry of Education of Design and Electromagnetic Compatibility of High-Speed Electronic Systems, Shanghai Jiao Tong University, Shanghai 200240, China

Corresponding author: Can Xiong (candemailbox@sjtu.edu.cn)

This work was supported by the National Key Research and Development Program of China under Grant 2019YFB2204703.

ABSTRACT A diagnosing method for phased antenna array element failures is proposed. The element excitation amplitudes and phases are reconstructed by a compressed sensing based approach, in which the radiated electric fields of the array are sampled by a single fixed receiving antenna. The diagnosing can be processed when the phased array is still in service. Particularly, it can be specialized for detecting faults only. Element excitation phases are designed to follow Bernoulli distribution, which is difficult to be realized in conventional geometric sampling methods. It is capable to provide effective and simultaneous detection for different types of failures with phase control means that are simpler comparing with other methods in which excitation phase adjustment is required. Especially, a two-step detection strategy is proposed to effectively detect phase failures due to faultily short-circuited phase shifters. Numerical results illustrate the effective sensing range of a single receiving antenna. Full-wave simulations validate the diagnosing performance in the presence of mutual couplings between array elements.

INDEX TERMS Phased array antenna, array diagnosis, phase shifter, compressed sensing, Bernoulli distribution.

I. INTRODUCTION

Phased array antennas are widely used in many engineering applications such as radar, sonar, and biology systems [1]. With the development of wireless communications, more applications appear in satellite, remote sensing and cellular communications recently [2]. Phased arrays usually consist of a large number of antenna elements. Due to the harsh operation environment, the occurrence of element errors and failures is inevitable, which will deteriorate the array performance. Owing to numerous sources of defects, it is difficult to detect them at one time. To preserve the performance of phased arrays, detecting different types of defects in a fast and accurate manner is valuable. It is meanwhile the preprocessing procedure of approaches to compensate a phased array with a small number of failed elements by adjusting excitations of other normal elements [3].

The associate editor coordinating the review of this manuscript and approving it for publication was Qingchun Chen.

The detection of defects in the whole array under test (AUT) can be casted into a problem of reconstructing the complex excitations of antenna elements. The backward propagation method transfers near field radiation data to the array aperture to verify element excitations [4]. In matrix methods [5], [6], excitations and near field data are written in a matrix form, so that the reconstruction is equivalent to solving the inverse problem. Neural network methods apply far field data to build training sets. Defective elements are located by properly selected network parameters [7], [8]. By microwave holography methods, the hologram on the array aperture is obtained from the measured far field pattern [9], [10]. Methods dealing with arbitrary distributions of array elements are reported in [11], [12]. Singular value decomposition (SVD) has been applied to find the solution. A low degree polynomial kernel has been developed for fast diagnosing by support vector machine (SVM) [13]. Other than on-off failures, partial faults have been handled in [14]. In those methods, a large number of measurements are required, which decreases the total efficiency. Fast

diagnosis methods dealing with digital phase shifter failures in phased arrays are proposed in [15]–[17]. Independent data are obtained by shifting antenna excitation phases [15]. The mutual coupling technique (MCT) is used to identify element phase failures by measuring adjacent elements [16], [17]. It is assumed that array elements are uniform and the mutual coupling among adjacent elements is the same. The measuring antenna is fixed during failure detection. Although the measuring procedure is simple, it still requires the measurement number to be far larger than the total number of phased array elements. The control of excitation phases is also complicated.

In the last decade, detection approaches based on compressed sensing (CS) [18]–[31] have been popular, by which the required number of measurements can be largely reduced. According to CS theory, unknown sparse signals can be retrieved from a small set of observations [32], [33]. In [19], [20], the sparse vector is generated by subtracting a reference excitation vector from AUT excitation vector. The sparse vector is firstly obtained and then commonly adopted in later CS based detection approaches. A regularization has been added to solve the optimization from measured near field data. Random partial Fourier matrices (RPFMs) have been used for the retrieval via far field data. The Bayesian CS based framework is proposed to provide reliable detections in [18], [26]. In order to detect AUT via magnitude data only, approximations and modifications are provided in [21], [24]. Convex optimizations for different configurations are assessed in [28], [29]. The measurement number is further reduced by sparsity promotion methods [30]. The sampling in those methods is performed at different receiving locations. The radiated fields are sampled in the phase domain in [31] to avoid probe shifting errors. However, only on-off failures are detected, partial failures and phase failures cannot be diagnosed. The above methods are mainly designed to detect only excitation failures or aperture field distributions. Although uncorrelated measurements can be obtained, the way to regulate the detection system is quite limited since the required condition on the sensing matrix is usually satisfied approximately using random Gaussian distribution only.

In this paper, a detecting method for different types of faults in phased arrays is proposed. It applies near field data for detection, which is practical in very large arrays. After the establishment of sparse excitation vectors, electric field data are sampled in the phase domain by a single fixed antenna [31]. The way of constructing the detection system is different. Since data can be sampled at only one fixed location, it simplifies the measurement process which is most time-consuming in diagnosing. Besides, it enables new ways to design the CS based detection system, in which entries in the sensing matrix can be managed flexibly by utilizing different random distributions. Via controlling element excitation phases, requirements of CS are satisfied by binary random matrices whose entries follow Bernoulli distribution. It is different from existing detection methods by which binary random matrices are hard to build. Therefore, Bernoulli distribution can be easily and strictly achieved in the proposed method. In traditional detection schemes that directly apply CS for real number analysis, excitation phase failures are difficult to be identified, since the phase information is not included in the unknown excitation vector to be retrieved. Not to mention that a faulty element may contain both amplitude and phase defects. In the proposed method, the original unknown excitation vector is split to real parts and imaginary parts to form a new vector whose entries are all real numbers. Both amplitude and phase failures can be distinguished and then detected simultaneously. Convex and non-convex optimization are both performed and compared. The non-convex one indicates better capability.

A q-bit digital phase shifter contains q phase-shifting stages. Phase control is realized by short-circuiting some phase-shifting stages according to the control signal. Typical phase failures are usually caused by faultily short-circuited stages in phase shifters. It is important to note that these short-circuiting phase failures coincide with some of the normal phase states, so that the effect of these failures is invisible and cannot be detected by conventional methods. A two-step detection is applied in consideration of this kind of failures. Firstly, a special control approach of phase shifters is designed to discover those faults at one single bit (usually the highest bit). Then, possible short-circuiting failures at the rest bits are diagnosed along with other kinds of failures. The measurement number is small compared with the total number of possible fault cases.

Compared with methods sampling data at different spatial locations, the proposed method takes advantages of the adjustable excitation phases in phased arrays. The independence of measured data and the constraints of CS can be satisfied in a more rigorous way by regulating array element excitation phases properly. The phase control is easier and the types of detectable failures are also extended.

This paper is organized as follows. In Section II, the detection system is formulated and analyzed. The diagnosing for different defects is illustrated in Section III. In Section IV, numerical examples are presented to show the detection performance in detail. Full wave simulations are implemented in Section V to validate the behavior of proposed method in a more practical case taking into account of the mutual coupling effect.

II. THE DIAGNOSING PROBLEM

The radiation properties of a phased antenna array, such as the main beam direction, gain, and sidelobe levels, mainly depend on three factors: the types of array elements, their geometric distributions, and complex excitations. Due to the presence of errors and failures, the array performance may be degraded. The degradation can be expressed by the deviation of practical element excitations from the idea ones. To diagnose a phased array, a main task is to retrieve the excitations from observed data.

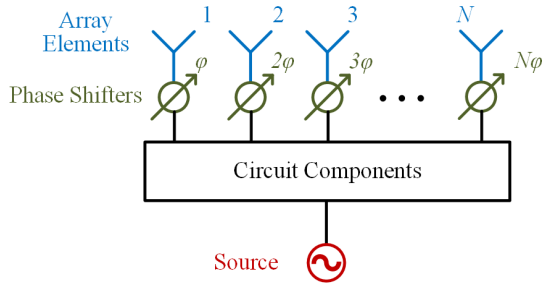

(a) An N element linear phased antenna array.

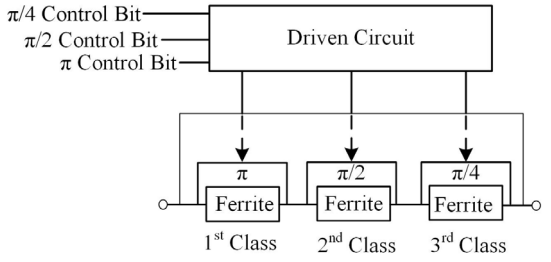

(b) A 3-bit digital ferrite phase shifter.

FIGURE 1. An example of a phased antenna array and a 3-bit digital phase shifter.

A. CLASSIFICATION OF EXCITATION DEFECTS

A phased antenna array is mainly composed of three parts: radiation antenna elements, phase shifters with control circuits, and excitation sources along with the feeding network, as shown in Fig. 1(a). The feeding network may contain amplifiers, isolators, power dividers, and attenuators, etc. Discrete digital phase shifters are commonly applied in large phased arrays owing to the convenience and flexibility to control element phases. A 3-bit digital phase shifter is shown in Fig. 1(b). It is a 3-stage circuit, each stage controlled by a binary signal, with "0" corresponding to the short-circuiting state and "1" corresponding to the phase-shifting state. The number of achievable phase states and the minimum phase shift are $L = 2^3 = 8$ and $\Delta\varphi = 2\pi/2^3 = 45°$, respectively.

Excitation defects can be clarified into two types: amplitude defects and phase defects. For amplitude defects, fabrication tolerances and short-circuited electronic devices in each channel lead to abnormal element amplitudes. The open-circuiting and breakdown of devices and transmission lines will disconnect those corresponding elements and result in zero amplitudes.

There are two typical types of phase defects. The first one is shifting errors caused by inaccurate length of transmission lines and phase shifter errors. It causes abnormal phase shift. The second one is called partial phase failure, in which one or more stages in a phase shifter remain short-circuited because of failures. When a partial phase failure occurs at one stage, it coincides with those normal phase states with a "0" control bit of the same stage. In other words, in these phase states, the partial phase failures cannot be detected since it is difficult to distinguish whether the short-circuiting is due to a failure or due to the control signal "0".

To summarize and simplify formulations, we divide all defects into two categories: on-off failures and partial defects. Failures resulting in zero excitations are termed as on-off failures. The rest defects that lead to abnormal amplitudes, phase shift deviations, and partial phase failures are named as partial defects. The two types of defects can be characterized from their excitations. The way to detect both on-off failures and partial defects will be presented in Section III.

B. VIRTUAL ARRAY AND ARRAY MANIFOLD

The electric field of an N element phased array can be expressed by the superposition of element electric fields, given by (1):

$$\vec{E} = \sum_{n=1}^{N} c_n \vec{E}_n = \sum_{n=1}^{N} b_n e^{-j\varphi_n} \vec{E}_n \tag{1}$$

in which c_n is the complex excitation of the n-th element composed of amplitude b_n and phase φ_n. $\vec{E}_n$ is the complex element electric field factor at the receiving point.

An assumption is made that the number S of defective elements is small with respect to the total element number N. Suppose a failure-free reference array occupies the same configuration with AUT except for excitations. The differences of array excitations between the reference and AUT form a sparse excitation vector, and the difference array is referred to as the virtual phased array [19], [20]. Excitations of normal elements in AUT are the same with those in the reference array. As a result, they cancel each other during subtraction and those corresponding elements in the virtual array have zero excitations. Only defective elements possess non-zero excitations. Denote received fields of the reference array, AUT, and the virtual array with $\vec{E}^R$, $\vec{E}^A$, and $\Delta\vec{E}$, (1) can be rewritten as:

$$\Delta\vec{E} = \vec{E}^R - \vec{E}^A = \sum_{n=1}^{N} \Delta c_n \vec{E}_n \tag{2}$$

where the superscript 'R' denotes the reference and 'A' denotes AUT. Δc_n is the complex excitation of the n-th element in the virtual array, which is given by:

$$\begin{aligned}\Delta c_n &= b_n^R e^{-j\varphi_n^R} - b_n^A e^{-j\varphi_n^A} \\ &= \left(b_n^R \cos\varphi_n^R - b_n^A \cos\varphi_n^A\right) - j\left(b_n^R \sin\varphi_n^R - b_n^A \sin\varphi_n^A\right)\end{aligned} \tag{3}$$

Since S elements in the virtual array have non-zero excitations, the virtual array is considered as a sparse array with only S antenna elements radiating fields.

To retrieve complex excitations of AUT, a linear detection system is formulated in (4):

$$\begin{aligned}&\mathbf{y} = \mathbf{A}\mathbf{x} + \mathbf{e} \\ &\mathbf{A} \in \mathbb{C}^{M\times N}, \quad A_{mn} = E_{mn} e^{-j\varphi_{mn}^R} \\ &\mathbf{y} = [y_1, y_2, \cdots, y_M] \in \mathbb{C}^{M\times 1}, \quad y_m = \sum_{n=1}^{N} \Delta c_{mn} E_{mn}\end{aligned}$$

$$\mathbf{x} = [x_1, x_2, \cdots, x_N] \in \mathbb{C}^{N\times 1},$$
$$x_n = b_n^R - b_n^A e^{-j\Delta\varphi_n} = \left(b_n^R - b_n^A \cos\Delta\varphi_n\right) + j\left(b_n^A \sin\Delta\varphi_n\right)$$
$$\mathbf{e} = [e_1, e_2, \cdots, e_M] \in \mathbb{R}^{M\times 1} \tag{4}$$

where $\mathbf{y}$ is the radiated field vector of the virtual array, M stands for the total measurement number, $\mathbf{x}$ is the vector of unknowns. The sensing matrix $\mathbf{A}$ is an $M \times N$ matrix of array manifold, and $\mathbf{e}$ is the noise vector. The entry A_{mn} of $\mathbf{A}$ is the product of the electric field factor E_{mn} of the n-th element at the m-th measurement and the corresponding ideal element excitation phase $e^{-j\varphi_{mn}^R}$ in the reference array. The entry x_n of the unknown vector $\mathbf{x}$ is formed by subtracting $b_n^A e^{-j\Delta\varphi_n}$ from the ideal excitation amplitude b_n^R of the n-th element, in which b_n^A refers to the actual excitation amplitude in AUT and $\Delta\varphi_n = \varphi_n^A - \varphi_n^R$ refers to the excitation phase difference of the n-th element. In this way, the ideal element excitation phases are included in matrix $\mathbf{A}$ to form a proper sensing matrix. The information of practical excitations of AUT are contained in the unknown vector $\mathbf{x}$.

C. SAMPLING STRATEGY

In CS based detection methods, properties of the sensing matrix are affected by the sampling strategy. There are two ways to regulate the sensing matrix. The traditional one is the geometric sampling by receiving fields at different positions or sampling radiation patterns at various angles in the far field. Independent data and the sensing matrix are controlled by the geometry distribution of measurement locations while excitations of array elements remain unchanged. Accordingly, in entry A_{mn}, the electric field factor E_{mn} varies along with the receiving location. Nevertheless, the ideal element excitation phase φ_{mn}^R is independent with measurement index m. Once the receiving location changes, while φ_{mn}^R stays constant, both the amplitude and phase of E_{mn} change. In fact, E_{mn} is proportional to $e^{-jkr_{mn}}/r_{mn}$ for far field measurements, in which k is the wavenumber and r_{mn} is the distance from the element to the receiving location. Thus, it is difficult to identify proper sampling positions so that entries in the sensing matrix can follow the required distributions.

Taking into account the agile beam steering property of phased arrays, a novel sampling strategy is to keep the receiving location fixed, rotate the array beam by different excitation phases, and record data during beam scanning. By this means, the electric field factor E_{mn} is independent with m, only the excitation phase φ_{mn}^R varies. If the phase adjustment schemes are carefully designed, it is possible to construct a proper sensing matrix $\mathbf{A}$. Different from the MCT method or other methods which require complicated and massive phase adjustments, the proposed method samples data in the phase domain in a simple and random manner. Thus, it is possible to detect failures while AUT is still in-service.

Except for being able to meet the required criterions for the sensing matrix, the phase domain sampling method provides an alternative way to design the sensing matrix. Since measurements are received at a fixed location, E_{mn} reduces to E_n that can be regarded as the weighting coefficient. It can be obtained via different approaches, such as computational EM methods, software simulations, and even on-site measurements. For instance, one can simulate the array and excite one element at once with excitation ''1''. Then, record the electric field at the fixed position to get one weighting coefficient E_n. After repeating the process N times, an $N \times 1$ coefficient vector can be obtained. The entire sensing matrix is the product of the excitation phase matrix and a diagonal weighting coefficient matrix:

$$\mathbf{A} = \mathbf{\Phi}\mathbf{\Psi} \tag{5}$$

in which $\mathbf{\Phi}$ is an $M \times N$ matrix whose entries are controlled by ideal element excitation phases, i.e., $\Phi_{mn} = e^{-j\varphi_{mn}^R}$, and $\mathbf{\Psi}$ is an $N \times N$ diagonal matrix whose diagonal elements are those weighting coefficients, that is, $\Psi_{nn} = E_n$.

In traditional geometric sampling methods, the detection system is usually governed by pattern multiplication theory or partial Fourier transform in the far field, and the mutual couplings among elements are not considered. The calculated matrix $\mathbf{A}$ is different from the practical case. If the entries in $\mathbf{A}$ are obtained by simulations or on-site measurements, it requires $M \times N$ times to measure them all. Besides, the constructed $\mathbf{A}$ is only valid for one single trial. The process is redundant and inefficient. In the proposed phase domain sampling, since the receiving antenna is fixed, it requires only N times to measure the entries. More importantly, for different trials and failure patterns, the sensing matrix $\mathbf{A}$ is valid once for all as long as the position of the receiving antenna remains unchanged.

III. EXCITATION RETRIEVAL BASED ON COMPRESSED SENSING

When applying CS for excitation retrieval, the restricted isometry property (RIP) condition which is the constraint on the sensing matrix $\mathbf{A}$ needs to be satisfied. In equation (4), if $\mathbf{A}$ satisfies RIP, the inverse problem $\mathbf{x} = (\mathbf{y} + \mathbf{e})\,\mathbf{A}^{-1}$ has a unique solution and it can be solved by sparse approximation algorithms even if the total number of measurements is less than the number of unknowns ($M < N$) [34]. However, verifying the RIP condition of a matrix is difficult. According to [35], $\mathbf{A}$ satisfies RIP provided that the measurement matrix $\mathbf{\Phi}$ and the sparse dictionary matrix $\mathbf{\Psi}$ are uncorrelated. Moreover, to successfully and accurately calculate $\mathbf{x}$, the number of measurement needs to obey [34]:

$$M \geq CS \ln(N/S) \tag{6}$$

in which C is a universal constant.

It is difficult to directly construct $\mathbf{\Phi}$ that is uncorrelated with $\mathbf{\Psi}$. Candés proved that $\mathbf{A}$ has high probability to satisfy the RIP condition if $\mathbf{\Phi}$ is a random Gaussian matrix that its entries follow the independent and identical Gaussian distribution [36,37]:

$$\Phi_{mn} \sim N\left(0, \frac{1}{N}\right) \tag{7}$$

Another choice of $\mathbf{\Phi}$ is the binary random matrix whose entries follow Bernoulli distribution that

$$\Phi_{mn} := \begin{cases} \frac{+1}{\sqrt{M}} \text{ with probability } \frac{1}{2}, \\ \frac{-1}{\sqrt{M}} \text{ with probability } \frac{1}{2}. \end{cases} \tag{8}$$

As is known in [38], using different random matrices in different application scenarios can enhance the performance of detection. In conventional spatial sampling methods, Gaussian distribution is commonly applied by measuring data at random receiving locations. Other random distributions are difficult to realize, since when changing the receiving locations, entries in $\mathbf{\Phi}$ change simultaneously. The modification of a single element at each time is inconvenient without affecting other elements. The choices of random distributions for constructing $\mathbf{\Phi}$ are restricted. In the proposed method, by using binary random matrices, excitation phase failures that cannot be diagnosed in [31] can be detected along with other kinds of failures. It will be presented in following subsections.

A. SCANNING MODE AND DETECTION MODE

According to Huygens' Principle, in order to reconstruct excitations of AUT, it is required to sample the electric field on a closed surface around it. For a phased antenna array, the fields can be sampled with a fixed probe with different excitation phases. If the array is able to scan in sufficiently wide directions, the information contained in phase domain sampling and in the geometric sampling are approximately equivalent. However, for a practical phased array using digital phase shifters, the range of achievable scanning directions is restricted and the scanning states are discrete. The available phase states are further limited when the array is in service, while excitation phases in a row, a column, or in a sub-array are usually altered simultaneously. Therefore, conventional non CS-based failure detection methods are not applicable because of insufficient sampling data in the phase domain. However, it is possible that the selected excitation phases satisfy requirements of the sensing matrix and contain enough information for defect detections using CS.

There are basically two diagnosing approaches for phased array antennas. One is to perform diagnosis when the phased array antenna is working and sample data during the scanning process. This method is referred as diagnosing in the scanning mode. The second one is referred as the detection mode. It is specially designed for performing diagnosis, where all phase states that phase shifters can provide are available to be controlled for the purpose of diagnosis. The detection performance of the two modes are obviously different.

In the scanning mode, the scanning directions in the achievable phase state space are randomly selected to make $\mathbf{\Phi}$ an approximate random Gaussian matrix. As a result, on-off failures, partial amplitude defects, and abnormal phase shifting can be detected. However, phase failures caused by short-circuiting of phase shifters cannot be detected. Besides, the design of $\mathbf{\Phi}$ is subject to much severe restriction because AUT has to maintain regular scanning.

In the detection mode, $\mathbf{\Phi}$ can be designed more flexibly to follow the expected random distributions. The phase failures due to faulty short-circuiting can be detected along with other defects. When adjusting excitation phases, short-circuited stages in faulty phase shifters produce non phase-shifting. The faulty stages cannot be distinguished from other normal working stages when the control signals are "0". In other words, if the control signal is "0", the corresponding stage is faulty or not cannot be verified. A special approach has to be applied to identify faultily short-circuited stages before diagnosing. It can be performed by properly chosen excitation phases.

Instead of random Gaussian matrix by which short-circuiting phase failures are difficult to be disclosed, the binary random matrix that follows Bernoulli distribution is capable in this situation. The binary entries in $\mathbf{\Phi}$ correspond to two different states of phase shifters with equal probability of 50%. The key point is to generate two independent states to implement the Bernoulli distribution, and meanwhile, each state should be effective to expose the possible failure information. Take 6-bit digital phase shifters as examples. It is possible to expose all phase failures only when the control code is "111111". Otherwise, the phase failures related to the "0" control bits are invisible. We can see that it is impossible to detect phase failures of all bits at a time. Because we have only one qualified code "111111". It is also the reason that the method presented in [31] cannot detect short-circuiting phase failures, since there are no qualified control codes using Gaussian random matrices.

A good strategy is to divide the control bits of phase shifters into two groups and carry out the detection in two steps. Separately, the failures associated with the first group are detected in the first step, whereas the failures with bits in the second group are detected in the second step. The bit diagnosed in the first step is called the *flag bit*. We choose the highest bit as the flag bit in the first group as an example, then all other lower 5 bits are assigned to the second group. In the first step, the two independent codes are "111111" and "100000", corresponding to two independent phase states. Apparently, the faulty short-circuiting phase failure at the highest bit is always visible with the two codes. Furthermore, because the two codes have the largest phase interval in this situation, the detection accuracy is also better, as will be verified with examples in later section.

After failures at the flag bit have been detected, their effect can be compensated by modifying the sensing matrix. Then in the second step, we can choose the two independent codes "111111" and "011111" to create the binary random sensing matrix. In fact, the binary values are achieved by the flag bit. It is obvious that short-circuiting related phase failures at lower 5 bits are all visible in this step, and can be detected by CS based methods.

B. SPARSE RECONSTRCUTION OF EXCITATIONS

In terms of (4), the entries of vectors and matrices in the detection system are all complex. However, CS based sparse reconstruction algorithms are commonly developed for real number analysis. If detecting amplitude failures only, either the real or imaginary parts of entries in the sensing matrix can be separated and applied alone. In phased antenna arrays, in order to detect both amplitude and phase defects, it is required to modify the detection system given by:

$$\begin{aligned}
&\tilde{\mathbf{y}} = \tilde{\mathbf{A}}\tilde{x} + \tilde{\mathbf{e}} \\
&\tilde{\mathbf{y}} = \begin{bmatrix} \mathrm{Re}\,(\mathbf{y}) \\ \mathrm{Im}\,(\mathbf{y}) \end{bmatrix} \in \mathbb{R}^{2M\times 1}, \quad \tilde{\mathbf{x}} = \begin{bmatrix} \mathrm{Re}\,(\mathbf{x}) \\ \mathrm{Im}\,(\mathbf{x}) \end{bmatrix} \in \mathbb{R}^{2N\times 1} \\
&\tilde{\mathbf{A}} = \begin{bmatrix} \mathrm{Re}\,(\mathbf{A}) & -\mathrm{Im}\,(\mathbf{A}) \\ \mathrm{Im}\,(\mathbf{A}) & \mathrm{Re}\,(\mathbf{A}) \end{bmatrix} \in \mathbb{R}^{2M\times 2N}, \quad \tilde{\mathbf{e}} = \begin{bmatrix} \mathbf{e} \\ \mathbf{z} \end{bmatrix} \in \mathbb{R}^{2M\times 1}
\end{aligned} \tag{9}$$

where $\mathrm{Re}\,(\cdot)$ is the real value operator, $\mathrm{Im}\,(\cdot)$ is the imaginary value operator, $\mathrm{Re}\,(x_n) = b_n^R - b_n^A \cos\Delta\varphi_n$ is the n-th entry of $\mathrm{Re}\,(\mathbf{x})$, and $\mathrm{Im}\,(x_n) = b_n^A \sin\Delta\varphi_n$ is the n-th entry of $\mathrm{Im}\,(\mathbf{x})$, $\mathbf{z}$ is an $M\times 1$ zero vector. Then, excitation amplitude and phase information of array elements are separated and are both contained in $\tilde{\mathbf{x}}$. After reconstructing $\tilde{\mathbf{x}}$, real and imaginary parts of $\mathbf{x}$ can be identified to determine amplitude and phase defects. This detection system can also be directly solved with existing CS based methods to detect phase failures.

The sparsity of the new unknown vector $\tilde{\mathbf{x}}$ is different. The sparsity S of the original vector $\mathbf{x}$ represents the total number of defective elements in AUT, whereas an impaired element may contain one of or both the amplitude and phase defect at the same time. If a defective element has amplitude defect only, it indicates one non-zero entry in vector $\tilde{\mathbf{x}}$. Otherwise, there are two non-zero entries in $\tilde{\mathbf{x}}$, corresponding to the real part and the imaginary part of the faulty excitation. Denote the new sparsity with $\tilde{S}$, which satisfies $\tilde{S} \leq 2S$. Once $\tilde{\mathbf{x}}$ is solved, the amplitude and phase defects can be determined by comparing with the ideal element excitations. After identifying faults in the flag bit in stage one, other types of failures will be detected at the same time in stage two, in which the results obtained in stage one are used as priori information.

A number of algorithms have been applied to achieve the sparse reconstruction, which can be mainly classified into two categories: convex optimizations and non-convex optimizations. The first theoretical method is possibly the l_0-minimization. Since $\tilde{\mathbf{x}}$ is $\tilde{S}$ sparse, it is intuitively to find the solution by minimizing the l_0-norm of $\tilde{\mathbf{x}}$. Nevertheless, l_0-minimization is NP-hard which is impractical. An equivalent solution via l_1-minimization is then proved and utilized [36]. In consideration of noisy observations, the optimization problem can be illustrated as

$$\min_{\tilde{\mathbf{x}}\in\mathbb{R}^{2N\times 1}} ||\tilde{\mathbf{x}}||_1 \text{ subject to } ||\tilde{\mathbf{y}} - \tilde{\mathbf{A}}\tilde{x}||_2^2 \leq \varepsilon \tag{10}$$

The optimization in (10) is a quadratically constrained linear program. A commonly used convex optimization algorithm is basis pursuit de-noising (BPDN), where its standard formulation is given by [39]:

$$\min_{\tilde{\mathbf{x}}\in\mathbb{R}^{2N\times 1}} \frac{1}{2}||\tilde{\mathbf{y}} - \tilde{\mathbf{A}}\tilde{x}||_2^2 + \tau||\tilde{\mathbf{x}}||_1 \tag{11}$$

Suppose that the noise is Gaussian white noise with standard deviation σ. The left part of (11) is an l_2-norm used to minimize the reconstruction error while the right part is an l_1-norm to facilitate the sparse solution by enforcing the small components in $\tilde{\mathbf{x}}$ to be 0. The regularization parameter τ is non-negative used to balance the error and the sparsity. If $\tilde{\mathbf{A}}$ is normalized, $\tau = \sigma\sqrt{2\log(P)}$, where P is the cardinality of $\tilde{\mathbf{A}}$, namely $P = N$. If the restricted isometry constant (RIC) δ_{2S} satisfies $\delta_{2S} < \sqrt{2} - 1$ and $||\mathbf{e}||_2 \leq \varepsilon$, the solution $\hat{\mathbf{x}}$ of (11) satisfies

$$\begin{aligned}
&||\hat{\mathbf{x}} - \tilde{\mathbf{x}}||_2 \leq C_0\frac{||\hat{\mathbf{x}} - \tilde{\mathbf{x}}||_1}{S^{1/2}} + C_1\varepsilon \\
&C_0 = \frac{2[1 + (\sqrt{2}-1)\delta_{2S}]}{1 - (\sqrt{2}-1)\delta_{2S}}, \; C_1 = \frac{4(\sqrt{1+\delta_{2S}})}{1 - (\sqrt{2}-1)\delta_{2S}}
\end{aligned} \tag{12}$$

The inequality in (12) demonstrates the stability of BPDN that the $\tilde{S}$-sparse vector $\tilde{\mathbf{x}}$ can be recovered with limited error. The error can be divided into two parts, the left one is associated with the best $\tilde{S}$-term approximation residual and the right part is associated with the noise level ε. Inequality (12) can be satisfied if (6) is satisfied. Then, a regular way to accomplish the optimization is to convert BPDN into a quadratic program, which avoids dealing with negative values [40].

In addition to the aforementioned l_p-norms where p is an integer, the unconstrained l_p-minimization where $0 < p < 1$ is an alternative approach which is usually applied to handle noisy cases. Its objective function is given by substituting the l_1-norm by the l_p–norm

$$\min_{\tilde{\mathbf{x}}\in\mathbb{R}^{2N\times 1}} \frac{1}{2}||\tilde{\mathbf{y}} - \tilde{\mathbf{A}}\tilde{x}||_2^2 + \tau||\tilde{\mathbf{x}}||_p^p \tag{13}$$

Similarly, τ is a regularization coefficient that reweights the proportion of the sparsity $\tilde{S}$ and the retrieved error. The reconstruction error of (13), denoted by $||\hat{\mathbf{x}} - \tilde{\mathbf{x}}||_2^p$, is bounded as well

$$||\hat{\mathbf{x}} - \tilde{\mathbf{x}}||_2^p \leq C_2||\hat{\mathbf{x}} - \tilde{\mathbf{x}}||_2^p + C_3\varepsilon^p \tag{14}$$

where C_2 and C_3 are local constants associated with RIP and $\tilde{S}$ [25]. The optimization in (13) is non-convex resulting in the retrieved vector $\hat{\mathbf{x}}$ a local minimum. The iterative reweighted least square (IRLS) algorithm is commonly used to converge the iteration error to provide better detection accuracy [25], [41].

IV. NUMERICAL RESULTS

In this section, 10×10 planar arrays are applied. The antenna elements are confined as isotropic antennas. The central operating frequency is 2.4 GHz. Array elements are equally distributed with $d = \lambda/2$ and excited with uniform excitation amplitude, in which λ is the operating wavelength. 6-bit digital phase shifters are applied. A single fixed receiving probe is

placed in the near field region of AUT to collect electric field data. Gaussian white noise is added to the received electric fields of AUT. The signal-to-noise ratio (SNR) is 30 dB.

A hypothesis is made that at most 20% of total elements may contain defects. The number and locations of faulty elements are randomly selected in each trial. A defective element may contain one of or both the on-off failure and partial failures. Faulty levels of amplitude and phase are randomly selected. The partial amplitude failure is ranging from 10% to 80% of the normal excitation amplitude. The minimum partial phase failure that can be detected is assumed to be the same as the minimum phase shift that a phase shifter can produce, corresponding to the lowest control bit. For 6-bit shifters, it is $\Delta\alpha = 2\pi/2^6 = 5.625°$. A partial phase failure due to short-circuiting is $\Delta\alpha \cdot k_s$, where k_s is the short-circuited stage in the phase shifter.

The overall performance of detection is evaluated via mean square errors (MSE), $\text{MSE} = 10\log_{10}(|\mathbf{x}^A - \mathbf{x}^D|_2^2/N)$, where $\mathbf{x}^D$ is the retrieved complex excitation vector. If MSE of one trial is less than -30 dB, the detection is considered successful for all defects. 1000 trials are performed to obtain the average rate of successful recovery (RSR). The detection performance per element is evaluated by the reconstruction error ratio $\left|\left(x_n^A - x_n^D\right)/x_n^R\right|$ and the successful detection rate (SDR), in which x_n^D and x_n^R denote the retrieved excitation and the failure-free excitation of the n-th element, respectively. If $\left|\left(x_n^A - x_n^D\right)/x_n^R\right|$ is less than a threshold value of 0.1, the element excitation is successfully detected.

A. DETECTION RESULTS IN THE SCANNING MODE

The minimum discrete interval of the scanning angle is approximately $\theta_{\min} \approx \arcsin(\Delta\alpha \cdot \lambda/2\pi d) = 1.79°$. Suppose the maximum scanning angle is $\theta_{\max} = 45°$, the scanning range of AUT is from $+45°$ to $45°$. Thus, there are 50 scanning states available in one direction. If AUT scans in both azimuth and elevation directions, a scanning angle depends on a pair of scanning states. By randomly selecting the pair in the available scanning ranges, the independent electric fields can be received and the condition on the sensing matrix can be roughly satisfied.

The detection results according to different number of defects and measurements are given in Fig. 2. Different types of defects are verified at the same time except for phase failures caused by short-circuiting. The single receiving probe is positioned 1.5 wavelength away from the midpoint of the right side of AUT. The solid lines denote results calculated by non-convex optimizations using IRLS algorithm and the dash lines denote results calculated by convex optimizations using BPDN. Non-convex optimizations reveal better detection accuracy than the convex ones in the same configuration. Therefore, the RSR is poor if the number of faulty elements exceeds 15. It is mainly due to two reasons. Firstly, AUT works in regular scanning mode, the element excitation phases in rows and columns are varied linearly. Hence, the un-correlation property of columns in $\mathbf{\Phi}$ is not

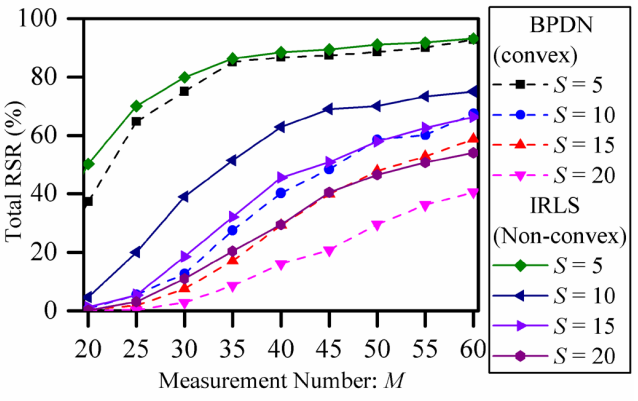

FIGURE 2. Total RSR according to $S = 5, 10, 15, 20$ against different number of measurement by BPDN (convex) and IRLS (non-convex) when AUT is in-service and the detection is in scanning mode.

satisfied rigorously. Secondly, the probe is placed very close to AUT, so that it lies in the near field regions of some antenna elements and in the far field regions of other elements. The magnitudes of the radiated fields at the probe by the two kinds of elements are hugely different.

The average element SDR is shown in Fig. 3 to demonstrate the effective sensing range of the probe in scanning mode. Those elements whose SDR are smaller than 85% are not displayed (they are denoted by blue squares in figures for a better resolution). In Fig. 3(a), the probe is placed 1.5 wavelength away from the midpoint of the right side of AUT. Its effective sensing range is nearly half a circle. If the probe is placed 1.5 wavelength away from the top right corner of AUT, the effective sensing range is nearly a quarter section of a circle. Although the detection accuracy in scanning mode is limited, it can be used for early-warning by properly designing alarm strategies in an on-site way.

B. DETECTION RESULTS IN THE DETECTION MODE

In the detection mode, all kinds of defects listed in this paper will be detected. Phase failures caused by short-circuiting and occurred at the flag bit are firstly detected in stage one. The highest bit is chosen as the flag bit. AUT may contain other kinds of defects at the same time. The binary "1" is represented by the control code of "111111" and the binary "0" is represented by "100000" in this stage. The detection results in a single trial are shown in Fig. 4. Although other phase defects are not detected precisely, phase failures of the flag bit have been identified correctly which will be used in the next stage.

In stage two, errors caused by phase failures of the flag bit are compensated in the sensing matrix in advance, according to diagnostic results in stage one. In this stage, the binary "1" is represented by "111111" and the binary "0" is represented by "011111". Possible phase defects of the rest five bits are exposed. Those defects along with other amplitude defects will be detected simultaneously. The detection results are shown in Fig. 5. Fig. 5(a) depicts the performance of

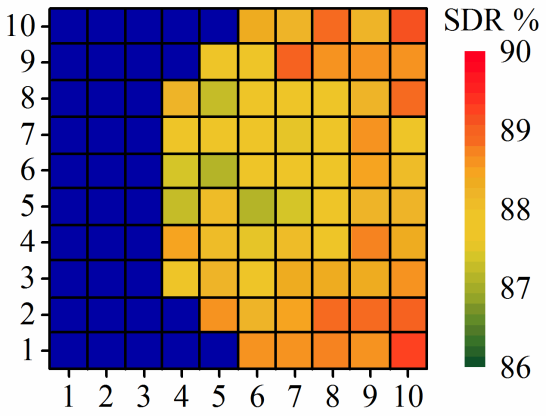

(a) SDR of each array element whereas the measuring location is 1.5 wavelength away from the midpoint of the right side of AUT.

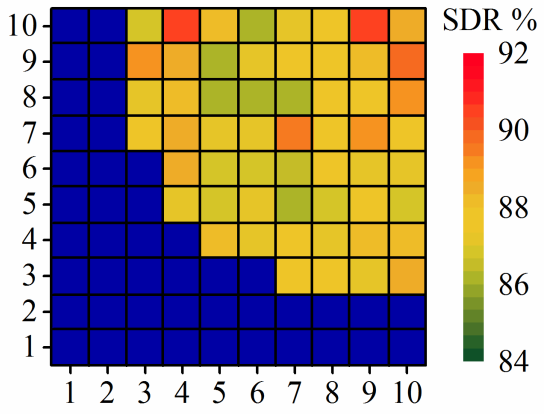

(b) SDR of each array element whereas the measuring location is 1.5 wavelength away from the top right corner of AUT.

FIGURE 3. The performance of detecting array element excitations at one single fixed location in the scanning mode when AUT is still working.

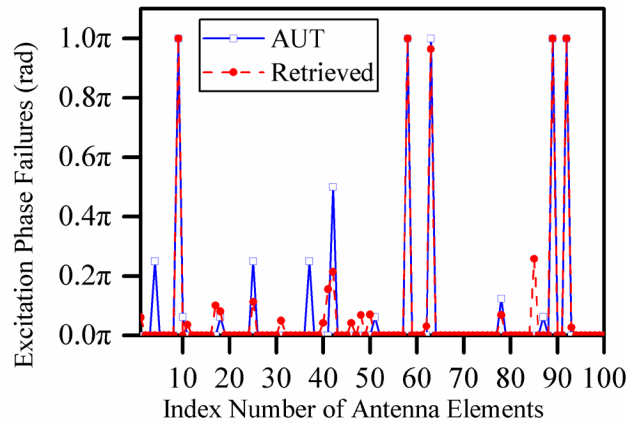

FIGURE 4. Element excitation phases failures detection of the highest control bit in detection mode in stage one.

amplitude failure detection. Both on-off failures and partial defects can be detected. Phase failures of the rest lower five bits are accurately recovered, as depicted in Fig. 5(b).

The average SDR of elements in the detection mode are given in Fig. 6. The AUT changes to a square array consisting of 24×24 elements. Since element excitation phases are randomly determined in the detection mode, requirements

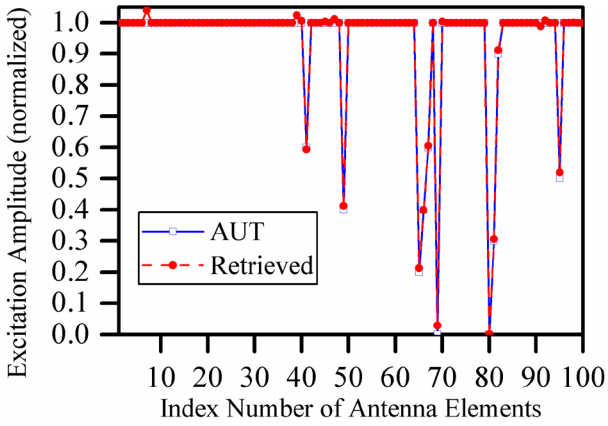

(a) Amplitude defects detections.

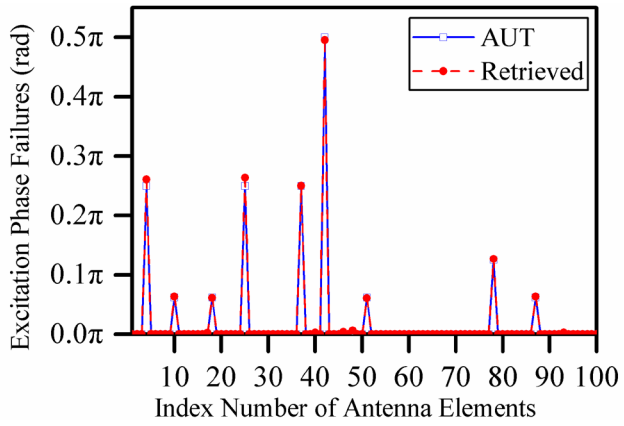

(b) Phase defects detections.

FIGURE 5. Element excitation amplitudes and phase defects diagnosis in the detection mode in stage two.

of the sensing matrix are satisfied more strictly. As a result, the effective sensing range of the single probe is extended. The shapes of effective sensing ranges in both the corner and the midpoint cases are in accordance with Fig. 3. The shape of the sensing range of a single probe is affected by two factors. One is the location of the receiving probe. The other is the type of antenna elements, which relates to different radiation pattern [31]. For large arrays, several probes can be placed at proper positions to preserve the accuracy according to the actual situation.

V. SIMULATION RESULTS

A 10×10 planar array along with one single receiving antenna have been simulated via HFSS shown in Fig. 7. The array elements and the receiving antenna are all bow-tie antennas with identical structures. Array elements are uniformly distributed with $d = \lambda/2$. The receiving antenna is located 1.5 wavelength away from the midpoint of the right side of AUT, so that all elements in AUT are in the effective sensing range of the measuring antenna. The central frequency is 3 GHz.

6-bits digital phase shifters are used. To simplify simulations, phase shifters are not directly implemented into the array. Instead, the phase shifting functions are realized

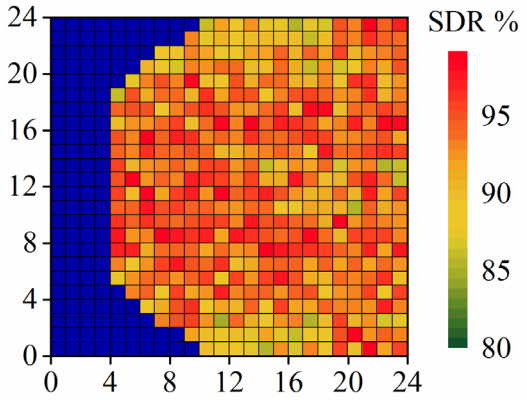

(a) SDR of each array element when the measuring location is 1.5 wavelength away from the midpoint of the right side of AUT.

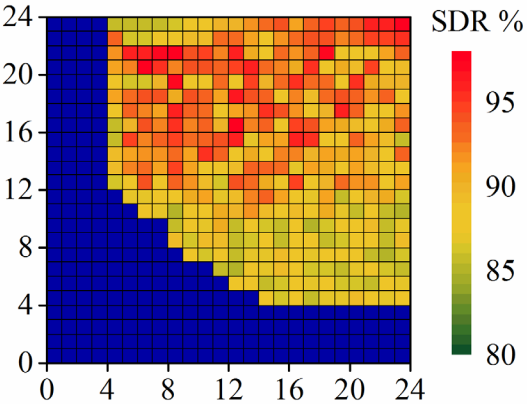

(b) SDR of each array element when the measuring location is 1.5 wavelength away from the top right corner of AUT.

FIGURE 6. The detection results of element excitations measured at one single fixed location in the specialized detection mode for 24×24 planar arrays.

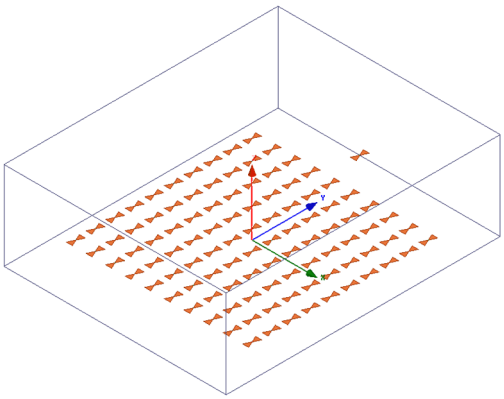

FIGURE 7. The geometric distribution of a 10×10 planar bow-tie array.

by editing the phases of the excitation sources of antenna elements. For the reference array free of detects and errors, the phase shifting is set according to control bits of phase shifters. For AUT, faulty excitation phase values are randomly produced as well as the locations of corresponding defective phase shifters. Phase shifting of other normal elements are the same with those in the reference array.

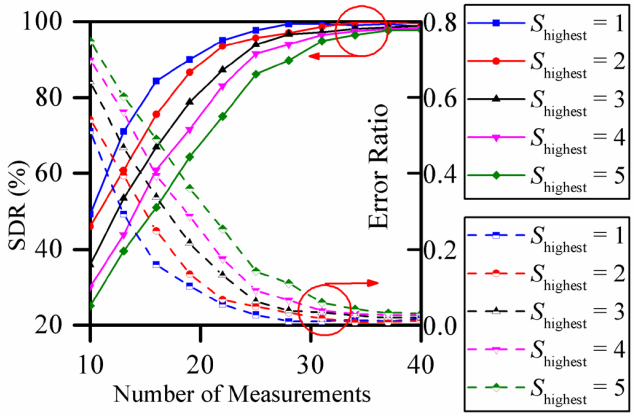

(a) Results according to different number of measurements.

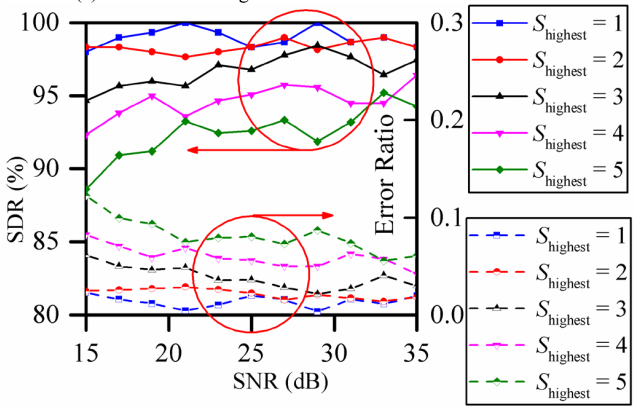

(b) Results at different SNR levels.

FIGURE 8. The detection results of phase failures caused by short-circuiting on the highest control bit in phase shifters in stage one in the detection mode.

The simulated system can be treated as a 101-port network whereas a port maps to an excitation port. Electric field contributions of antennas can be expressed by the 101×101 network scattering matrix $\mathbf{S}$. Denote the receiving antenna as the 101-th port, the scattering parameter $S_{101,n}$ in $\mathbf{S}$ can be applied to represent the electric field contribution of the n-th element in AUT at the receiving antenna. As a result, the diagonal entry E_n in $\mathbf{\Psi}$ can be denoted using $S_{101,n}$. In addition, the scattering parameters are linear with complex excitations of antennas which satisfy requirements of CS. Excitation phases are controlled in each trial. In this way, the mutual couplings among elements in AUT have been taken into account. The influence of the receiving antenna to AUT has been included in a similar way.

The detection results in stage one for identifying the flag bit are presented in Fig. 8. The highest bit is chosen as the flag bit firstly. The total number of defects is 20. The defective number of the highest bits in phase shifters is calculated from 1 to 5. (denoted by S_{highest} in the figure legend). Assume that there is a phase failure of the highest bit (denoted by $\Delta\varphi_n^A = \pi$). The failure is successfully detected if the normalized error ratio $\left(\Delta\varphi_n^D - \Delta\varphi_n^A\right)/\pi$ between the retrieved phase and that phase in AUT is smaller than the threshold

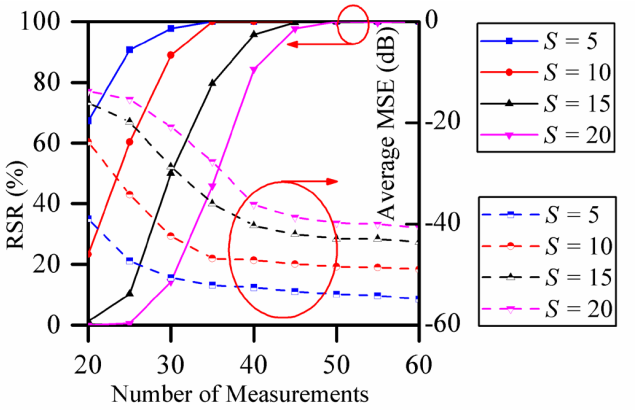

(a) Total RSR and MSE according to different measurement numbers.

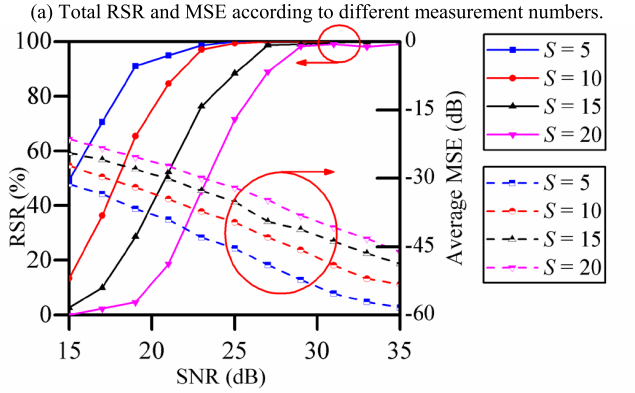

(b) Total RSR and MSE according to different SNR levels.

FIGURE 9. The detection results of all other kinds of defects in stage two in the detection mode.

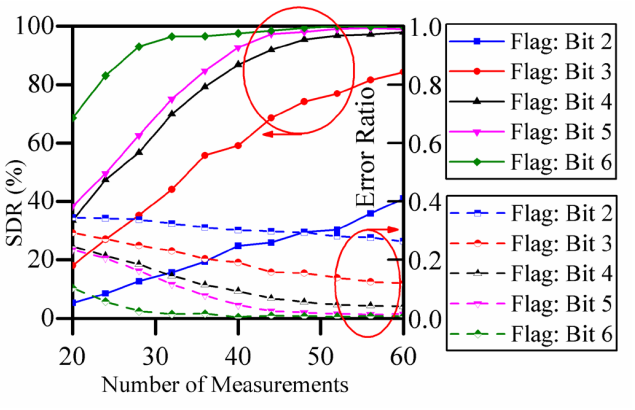

(a) Results in stage one by using different flag bits.

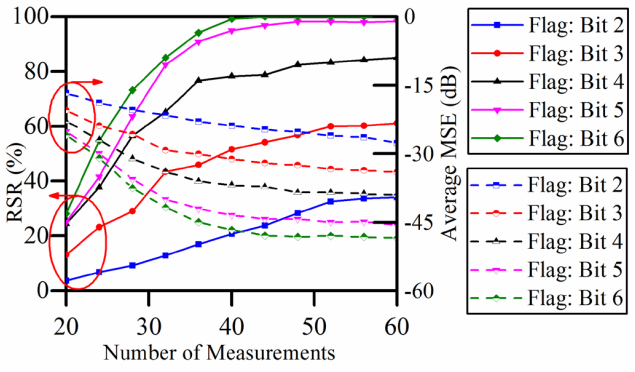

(b) Results in stage two by using different flag bits.

FIGURE 10. The detection results by using different flag bits in the detection mode.

of 0.1. 1000 trials are performed to calculate the average SDR.

Fig. 8(a) shows the SDR and error ratio according to different measurement numbers. If the measurement number exceeds 30, the SDR is larger than 90%. Fig. 8(b) shows the performance under different SNR levels. The results are less sensitive to noise since only one kind of failures are examined.

The results in stage two are shown in Fig. 9. All other kinds of defects except for those detected in stage one are diagnosed. Fig. 9(a) shows the total RSR and MSE according to different measurement numbers. A measurement number larger than 50 indicates an accurate detection which is in accordance with [42]. Fig. 9(b) shows the total RSR and MSE according to different SNR levels, the measurement number is confined as 50 in this case. If the SNR level is larger than 25 dB, RSR of 90% can be achieved. Although the detection occupies two stages, the total measurement number required is still less than the total number of array elements. In fact, for a 6-bit phase shifter, there are 6 kinds of defective phase states. If detecting failure states one by one, at least $6N$ trials should be performed. Moreover, more trials are required by traditional MCT methods since one element is diagnosed by no less than two adjacent elements.

Compared with those methods, the proposed method provides a more efficient detection with only a small number of measurements. Besides, the excitation phase management is easier to achieve in only two stages than feeding each array element one stage by one stage.

The aforementioned results examine the highest bit as the flag bit in stage one. Other bits can also be selected as flag bits with detection results shown in Fig. 10(a). The SDR is gradually decreased from bit 6 (highest bit) to bit 2. It is because a higher bit indicates a larger phase shifting interval between the two binaries, which is easier to be distinguished. Fig. 10(b) shows results in stage two when using other bits. It is in accordance with Fig. 10(a) that a higher flag bit reveals better detection performance.

VI. CONCLUSION

A method for detecting phased array antenna element failures is proposed. Radiated data are sampled in the phase domain by which only one receiving antenna is required. The receiving antenna is fixed during detection, only excitation phases are changed. It avoids the shifting error compared with conventional methods sampling data at different geometric positions. No additional operation on AUT is required, and the detection operation merely takes place on the controlling of phase shifters. A new detection system has been designed using binary random matrices to expose all types of failures, in which some phase failures caused by short-circuiting are hard to discover in other methods that need to control

excitation phases. Entries in the sensing matrix are created to follow Bernoulli distribution by regulating the excitation phases. Both on-off failures and partial errors can be detected with high accuracy. In addition to amplitude failures, this method is capable to diagnose phase failures especially those caused by faultily short-circuited phase shifters. The detection is divided into two steps. Short-circuiting phase failures in the flag bit are identified in the first step. The remaining bits are examined in the second step. Despite that short-circuiting phase failures may be buried in normal phase states, the detection is still accurate even in situations that amplitude faults occur at the same time. The required measurement number is much smaller than the total number of all possible faulty phase states.

Compared to phase faults detection methods in which phase shifter controlling is complex, the proposed method only needs simple phase control codes corresponding to two binaries states. Although only Gaussian distribution and Bernoulli distribution are applied in this paper, other sampling strategies may be feasible for detection in different situations if properly designed by sampling in the phase domain. The mutual coupling effect has been considered in the sensing matrix. Full wave simulation results validate the efficient detection performance.

REFERENCES

[1] R. J. Mailloux, *Phased Array Antenna Handbook*, 2nd ed. Norwood, MA, USA: Artech House, 2005.

[2] T. S. Rappaport, S. Sun, R. Mayzus, H. Zhao, Y. Azar, K. Wang, G. N. Wong, J. K. Schulz, M. Samimi, and F. Gutierrez, "Millimeter wave mobile communications for 5G cellular: It will work!" *IEEE Access*, vol. 1, pp. 335–349, 2013.

[3] M.-S. Kang, Y.-J. Won, B.-G. Lim, and K.-T. Kim, "Efficient synthesis of antenna pattern using improved PSO for spaceborne SAR performance and imaging in presence of element failure," *IEEE Sensors J.*, vol. 18, no. 16, pp. 6576–6587, Aug. 2018.

[4] J. J. Lee, E. M. Ferren, D. P. Woollen, and K. M. Lee, "Near-field probe used as a diagnostic tool to locate defective elements in an array antenna," *IEEE Trans. Antennas Propag.*, vol. AP-36, no. 6, pp. 884–889, Jun. 1988.

[5] L. Gattoufi, D. Picard, Y. R. Samii, and J. C. Bolomey, "Regularized matrix method for near-field diagnostic techniques of phased array antennas," in *IEEE Antennas Propag. Soc. Int. Symp. Dig.*, Nov. 2002, pp. 52–57.

[6] O. M. Bucci, M. D. Migliore, G. Panariello, and P. Sgambato, "Accurate diagnosis of conformal arrays from near-field data using the matrix method," *IEEE Trans. Antennas Propag.*, vol. 53, no. 3, pp. 1114–1120, Mar. 2005.

[7] A. Patnaik and C. Christodoulou, "Finding failed element positions in linear antenna arrays using neural networks," in *Proc. IEEE Antennas Propag. Soc. Int. Symp.*, Jul. 2006, pp. 1675–1678.

[8] S. Vigneshwaran, N. Sundararajan, and P. Saratchandran, "Direction of arrival (DoA) estimation under array sensor failures using a minimal resource allocation neural network," *IEEE Trans. Antennas Propag.*, vol. 55, no. 2, pp. 334–343, Feb. 2007.

[9] Y. Rahmat-Samii, "Microwave holographic metrology for antenna diagnosis," *IEEE Antennas Propag. Soc. Newsl.*, vol. 29, no. 3, pp. 5–16, Jun. 1987.

[10] J. Laviada Martinez, A. Arboleya-Arboleya, Y. Alvarez-Lopez, C. Garcia-Gonzalez, and F. Las-Heras, "Phaseless antenna diagnostics based on off-axis holography with synthetic reference wave," *IEEE Antennas Wireless Propag. Lett.*, vol. 13, pp. 43–46, 2014.

[11] A. Buonanno, M. D'Urso, M. Cicolani, and S. Mosca, "Large phased arrays diagnostic via distributional approach," *Progr. Electromagn. Res*, vol. 92, pp. 153–166, 2009.

[12] B.-K. Yeo and Y. Lu, "Fast detection and location of failed array elements using the fast SVM algorithm," in *Proc. 14th Int. Symp. Antenna Technol. Appl. Electromagn. Amer. Electromagn. Conf.*, Jul. 2010, pp. 1–4.

[13] A. Buonanno and M. D'Urso, "A novel strategy for the diagnosis of arbitrary geometries large arrays," *IEEE Trans. Antennas Propag.*, vol. 60, no. 2, pp. 880–885, Feb. 2012.

[14] B. Choudhury, O. P. Acharya, and A. Patnaik, "Bacteria foraging optimization in antenna engineering: An application to array fault finding," *Int. J. RF Microw. Comput.-Aided Eng.*, vol. 23, no. 2, pp. 141–148, 2013.

[15] S. Jun-ping, X. Ping, J. Shuai, and F. De-min, "Study on a fast measurement and identifying malfunction elements in phased array antennas," in *Proc. 2nd Asian–Pacific Conf. Synth. Aperture Radar*, Xi'an, China, Oct. 2009, pp. 591–594.

[16] Y. Neidman, R. Shavit, and A. Bronshtein, "Diagnostic of phased arrays with faulty elements using the mutual coupling method," *IET Microw. Antennas Propag.*, vol. 3, no. 2, p. 235, 2009.

[17] Y.-S. Chen and I.-L. Tsai, "Detection and correction of element failures using a cumulative sum scheme for active phased arrays," *IEEE Access*, vol. 6, pp. 8797–8809, 2018.

[18] G. Oliveri, P. Rocca, and A. Massa, "Reliable diagnosis of large linear arrays—A Bayesian compressive sensing approach," *IEEE Trans. Antennas Propag.*, vol. 60, no. 10, pp. 4627–4636, Oct. 2012.

[19] M. D. Migliore, "A compressed sensing approach for array diagnosis from a small set of near-field measurements," *IEEE Trans. Antennas Propag.*, vol. 59, no. 6, pp. 2127–2133, Jun. 2011.

[20] M. D. Migliore, "Array diagnosis from far-field data using the theory of random partial Fourier matrices," *IEEE Antennas Wireless Propag. Lett.*, vol. 12, pp. 745–748, 2013.

[21] B. Fuchs and L. Le Coq, "Excitation retrieval of microwave linear arrays from phaseless far-field data," *IEEE Trans. Antennas Propag.*, vol. 63, no. 2, pp. 748–754, Feb. 2015.

[22] M. D. Migliore, S. Costanzo, A. Borgia, D. Pinchera, and G. Di Massa, "Failures identification in a linear slot array using a sparse recovery technique," in *Proc. 8th Eur. Conf. Antennas Propag. (EuCAP)*, The Hague, The Netherlands, Apr. 2014, pp. 3214–3215.

[23] B. Fuchs, L. L. Coq, and M. D. Migliore, "Fast antenna array diagnosis from a small number of far-field measurements," *IEEE Trans. Antennas Propag.*, vol. 64, no. 6, pp. 2227–2235, Jun. 2016.

[24] A. F. Morabito, R. Palmeri, and T. Isernia, "A compressive-sensing-inspired procedure for array antenna diagnostics by a small number of phaseless measurements," *IEEE Trans. Antennas Propag.*, vol. 64, no. 7, pp. 3260–3265, Jul. 2016.

[25] T. Ince and G. Ogucu, "Array failure diagnosis using nonconvex compressed sensing," *IEEE Antennas Wireless Propag. Lett.*, vol. 15, pp. 992–995, 2016.

[26] M. Salucci, A. Gelmini, G. Oliveri, and A. Massa, "Planar array diagnosis by means of an advanced Bayesian compressive processing," *IEEE Trans. Antennas Propag.*, vol. 66, no. 11, pp. 5892–5906, Nov. 2018.

[27] M. E. Eltayeb, T. Y. Al-Naffouri, and R. W. Heath, Jr., "Compressive sensing for millimeter wave antenna array diagnosis," *IEEE Trans. Commun.*, vol. 66, no. 6, pp. 2708–2721, Jun. 2018.

[28] Y. Zhang and W. Wang, "Robust array diagnosis against array mismatch using amplitude-only far field data," *IEEE Access*, vol. 7, pp. 5589–5596, 2019.

[29] Y. Zhang, W. Wang, Y. Zhang, and W. Sun, "Convex optimization for array diagnosis using amplitude-only far field data in impulsive noise environment," *IEEE Access*, vol. 7, pp. 14035–14043, 2019.

[30] R. Palmeri, T. Isernia, and A. F. Morabito, "Diagnosis of planar arrays through phaseless measurements and sparsity promotion," *IEEE Antennas Wireless Propag. Lett.*, vol. 18, no. 6, pp. 1273–1277, Jun. 2019.

[31] C. Xiong, G. Xiao, Y. Hou, and M. Hameed, "A compressed sensing-based element failure diagnosis method for phased array antenna during beam steering," *IEEE Antennas Wireless Propag. Lett.*, vol. 18, no. 9, pp. 1756–1760, Sep. 2019.

[32] D. L. Donoho, "Compressed sensing," *IEEE Trans. Inf. Theory*, vol. 52, no. 4, pp. 1289–1306, Apr. 2006.

[33] E. J. Candes and M. B. Wakin, "An introduction to compressive sampling," *IEEE Signal Process. Mag.*, vol. 25, no. 2, pp. 21–30, Mar. 2008.

[34] E. J. Candè,"The restricted isometry property and its implications for compressed sensing," *Comp. Rendus Mathematique*, vol. 346, nos. 9–10, pp. 589–592, May 2008.
[35] J. Haupt, L. Applebaum, and R. Nowak, "On the Restricted Isometry of deterministically subsampled Fourier matrices," in *Proc. 44th Annu. Conf. Inf. Sci. Syst. (CISS)*, Princeton, NJ, USA, Mar. 2010, pp. 1–6.
[36] E. J. Candès and T. Tao, "Decoding by linear programming," *IEEE Trans. Inf. Theory*, vol. 51, no. 12, pp. 4203–4215, Dec. 2005.
[37] E. J. Candès, J. K. Romberg, and T. Tao, "Stable signal recovery from incomplete and inaccurate measurements," *Commun. Pure Appl. Math.*, vol. 59, no. 8, pp. 1207–1223, Aug. 2006.
[38] R. Baraniuk, M. Davenport, R. DeVore, and M. Wakin, "A simple proof of the restricted isometry property for random matrices," *Constructive Approximation*, vol. 28, no. 3, pp. 253–263, Dec. 2008.
[39] Z. Yang, C. Zhang, and L. Xie, "Robustly stable signal recovery in compressed sensing with structured matrix perturbation," *IEEE Trans. Signal Process.*, vol. 60, no. 9, pp. 4658–4671, Sep. 2012.
[40] S. S. Chen, D. L. Donoho, and M. A. Saunders, "Atomic decomposition by basis pursuit," *SIAM Rev.*, vol. 43, no. 1, pp. 129–159, Jan. 2001.
[41] Z. Lu, "Iterative reweighted minimization methods for ℓ_p regularized unconstrained nonlinear programming," *Math. Program.*, vol. 147, nos. 1–2, pp. 277–307, Oct. 2014.
[42] J. A. Rodriguez-Gonzalez, F. Ares-Pena, M. Fernandez-Delgado, R. Iglesias, and S. Barro, "Rapid method for finding faulty elements in antenna arrays using far field pattern samples," *IEEE Trans. Antennas Propag.*, vol. 57, no. 6, pp. 1679–1683, Jun. 2009.

CAN XIONG (Student Member, IEEE) was born in Guizhou, China, in 1989. He received the B.S. degree in information engineering from Shanghai Jiao Tong University, Shanghai, China, in 2013, and the M.S. degree in communication engineering from The University of Warwick, Coventry, U.K., in 2014. He is currently pursuing the Ph.D. degree in electronic engineering with Shanghai Jiao Tong University.

His current research interests include phased antenna array diagnosis, compressed sensing, and antenna array synthesis.

GAOBIAO XIAO (Member, IEEE) received the B.S. degree from the Huazhong University of Science and Technology, Wuhan, China, in 1988, the M.S. degree from the National University of Defense Technology, Changsha, China, in 1991, and the Ph.D. degree from Chiba University, Chiba, Japan, in 2002.

He has been a Faculty Member with the Department of Electronic Engineering, Shanghai Jiao Tong University, Shanghai, China, since 2004. His research interests are computational electromagnetics, coupled thermo-electromagnetic analysis, microwave filter designs, fiber-optic filter designs, phased arrays, and inverse scattering problems.